Pressure Distributions and Ultimate Bearing Capacity of Footings on Cohesionless soil under Double Eccentric Loads

by

A.K. Basu*

Introduction

BASED on theory and experimental results, several authors have suggested various emperical and semiemperical formulae for ultimate bearing capacities of footings on soils, viz, Bell (1915), Terzaghi (1943), Meyerhof (1951), Skempton (1951), Hansen (1961), Balla (1962). But very limited data of test results for footings are available for the solution of eccentric foundations. For eccentric footings, Meyerhof (1953) suggested the concept of effective contact width $B' = B-2e$, ultimate bearing capacity being represented by $q_e = qB'$, where $q = c\,N_{cq}+0.5B'_{\gamma}N_{\gamma q}$. This suggested procedure can be extended to a rectangular foundation with eccentricities in x and y axis, by applying correction for the shape factor which depends upon L'/B' ratio of the contact area, Meyerhof (1953).

Pressure distributions beneath a foundation play an important role on the studies of principal problems of soil mechanics. The stress distributions within the soil mass should be known in order to find out the total settlement of the foundations. The stresses are worked out even today following Boussinesq's method, Jumikis (1965). As such, measurement of soil vertical pressures both in vertical and horizontal planes are made to study the pressure distributions along with the study of ultimate bearing capacity of double eccentric footings on cohesionless soil in the present investigations.

Experimental set-up

Load tests on model footings were conducted in an experimental setup as shown in Figure 1. A reaction loading frame was made and the load application was done by means of hanger mechanism where lever arm ratios available were 5 and 2.50.

Six series of model footings of sizes 15 cm × 15 cm, 12.50 cm × 12.50 cm, 10 cm × 10 cm for square footings, 12.50 cm × 10 cm, 15 cm × 10 cm and 15 cm × 12.50 cm for rectangular footings, made of 3.80 cm to 5 cm thick wooden blocks were used, conforming rough rigid base. In all the footings semi-round impressions were made at the centres, and at four double eccentric points, $L/6$, $B/6$; $2L/6$, $B/6$; $L/6$, $2B/6$; and $2L/6$, $2B/6$.

For pressure measuring device, a selector switch arrangement had been devised (Figure 2a), to connect five pressure cells in one switch board with the use of banana plugs, bases and band switch knob to select each cell in

* Senior Lecturer in Civil Engineering, Regional Engineering College, Rourkela-8.

* The paper is open for discussion till March 1976.

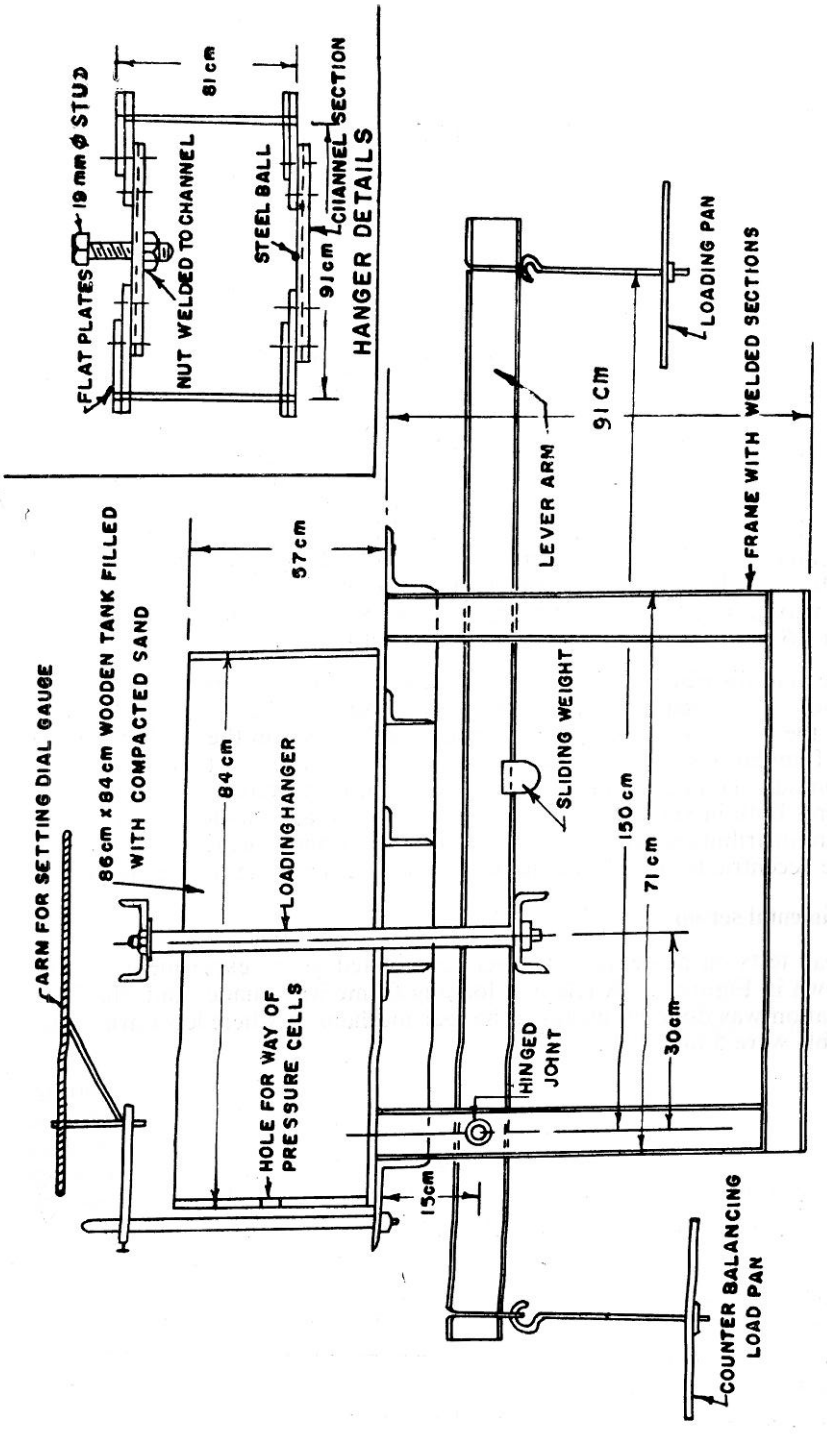

FIGURE 1 : Experimental set up

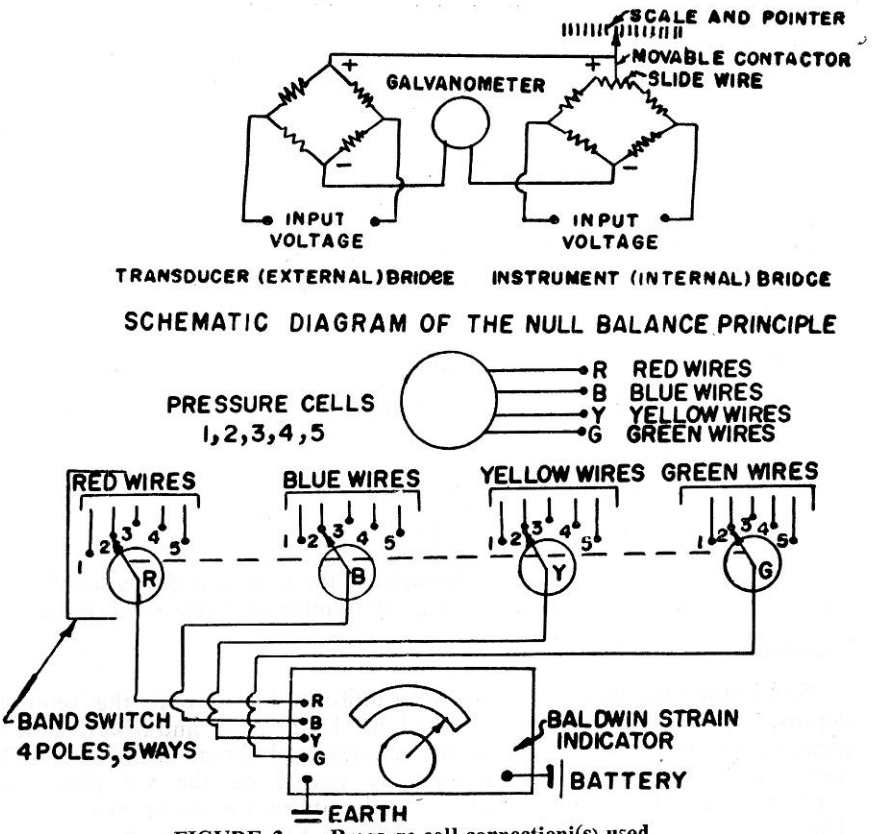

FIGURE 2a : Pressure cell connectioni(s) used.

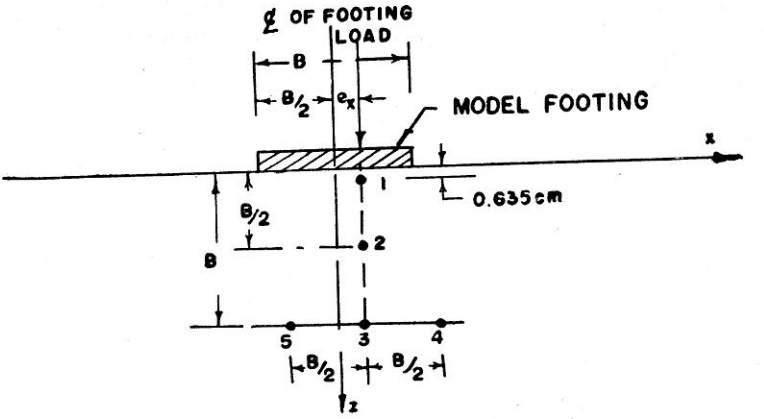

FIGURE 2b : Arrangements of Pressure cells below footing on same vertical plane.

circuit. The pressure cells were of Redshaw soil pressure transducer type having diameter 45 mm, thickness 15 mm, weight 44 gms, pressure range 0 to 7 kg/cm^2 and of sufficient sensitivity. The circuit was maintained through Baldwin type strain indicator which works on the null balance principles and measures strains by indicating the change of electrical resistance in SR_4 bonded wire strain gauges and eveready dry battery.

Each of the pressure cells had been calibrated by subjecting them to known pressures in triaxial compression testing machine. The strain indicator readings for nu'l deflections were taken at known pressure interval of 0.14 kg/cm² for pressures upto 1.40 kg/cm² and at 0.70 kg/cm² for pressures upto 4.20 kg/cm². These readings were taken both for pressure increase and decrease with the pressure cell suspended in air and also embedded in a small sack of sand tied round it. In either of the cases no appreciable difference was found. Calibration curves, showing the relationship between difference in indicator readings and pressure increments were drawn throughout the range of pressures for all the cells.

Dry cohesionless soil was used in the experiments which had following physical properties

Specific gravity	= 2.64
density	= 1.65 gm/cc,
relative density	= 60%,
angle of internal friction, ϕ	= 35°, and
Uniformity coefficient	= 2.22

This density was maintained throughout the tests and the value of ϕ at this density of soil had been found out by number of direct shear tests.

Experimental Procedure

Soil in the tank was compacted with uniform density upto the required depths. Five pressure cells marked as 1, 2, 3, 4 and 5 were used to measure normal stresses on horizontal planes at different locations. The arrangement of these cells, which were placed on the x-z plane and coplaner with the applied load, under the footings is shown in Figure 2b. These cells were covered with an aluminium plate while campaction were done as a precaution against displacements. On top of the finished soil surface model footing was placed. The hanger was brought over the footing with the displacement dial gauge set vertical on the stud. Lever arm was adjusted with a 10 mm. diameter steel ball to take loads. Loads from pressure cells were drawn outside through the hole provided in the tank and these were connected in the selector switch board. The circuit was made complete with the strain indicator and battery. Loads were applied *in steps with sufficient time allowance for steady record in the dial gauges,* until footings failed. Along with each load increment the pressure cell readings were obtained by selecting the cells by the operating knob attached to the selector switch.

Discussion of Test Results

Figures 3 and 4, show the load vs. settlement upto failure at different eccentric and centric load conditions. It is evident from these curves that the failure of the soil mass is intermediate between general shear and local shear failures. The soil density that was maintained in the tests was fairly dense and thus justifies the observed failure conditions.

Load settlement curves are drawn with tangent intersection method from which ultimate load carrying capacities of the footings are determined. Figures 5 and 6 show the variation of the ultimate load, determined as above, with the area of footings for different double eccentricities. It is

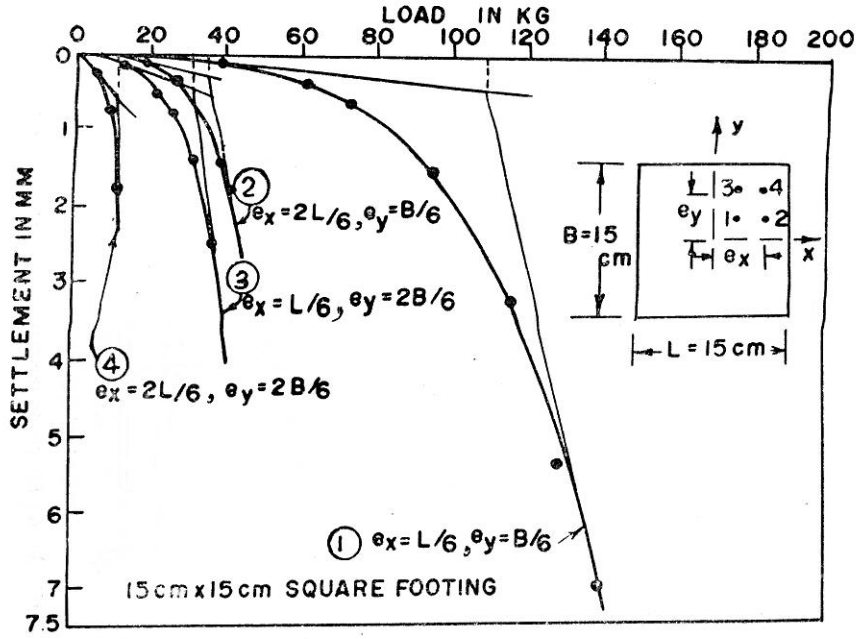

FIGURE 3 : Load settlement curve at different e_x/e_y.

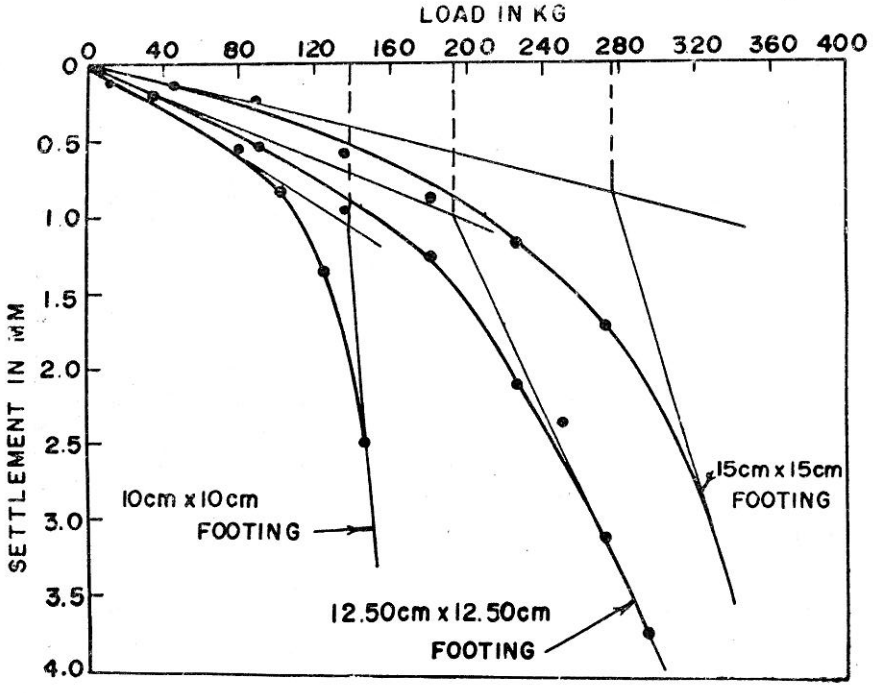

FIGURE 4 ; Load settlement curves for all central points of square footings.

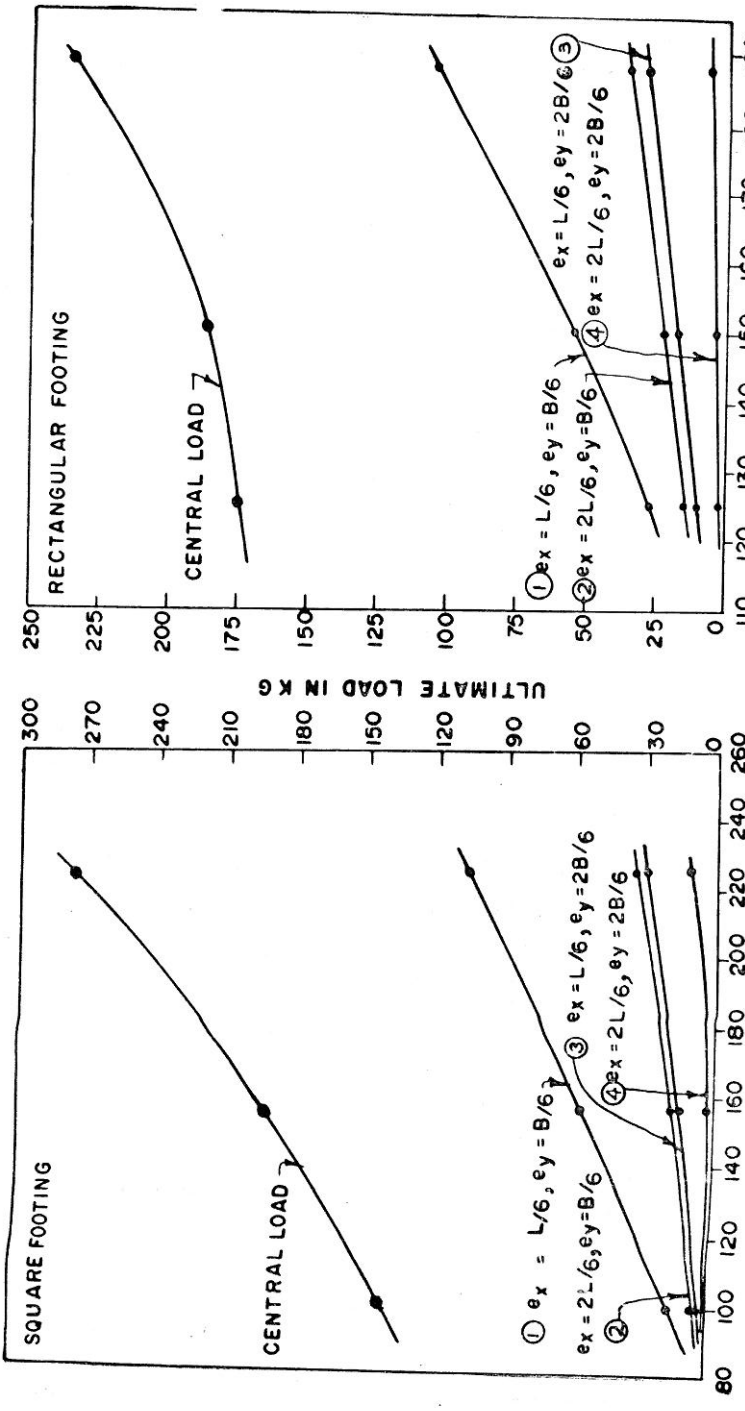

FIGURE 5 : Effect on ultimate loads at different e_x/e_y.

FIGURE 6 : Effect on ultimate loads at different e_x/e_y.

found that for any footing, whether square or rectangular, double eccentricity upto $e_x = L/6$, $e_y = B/6$, reduces the bearing capacity by a considerable amount. For footing area = 225 sq.cm., and at double eccentricity $e_x = L/6$, $e_y = B/6$, the bearing capacity is 107.96 kg. When compared to centric load the reduction is 61 percent. This reduction is found to vary between 55 to 70 percent when the footing area changes from 225 to 100 sq. cm. Ultimate bearing capacity gets further reduced when double eccentricity increases and at $e_x = 2\ L/6$, $e_y = 2B/6$; this reduction is about 95 to 99 percent compared to centric load. From the same figures, it is also seen that ultimate bearing capacity increases with the increase of footing areas when the double eccentricity is within $L/6$, $B/6$. Beyond this double eccentricity, the rate of increase of the ultimate bearing capacity is quite low with the increase of footing areas and at double eccentricity of $e_x = 2\ L/6$, $e_y = 2B/6$, this is too small. It is understood, therefore, that the size of footing has negligible effect on ultimate bearing capacity when the double eccentricity is beyond $e_x = L/6$, $e_y = B/6$. Ultimate bearing capacities from the test results are compared with the theoretical values, obtained with the effective contact area concept, following Terzaghi's theory and Meyerhof's theory (Table I). Terzaghi's ultimate bearing capacity is found to be conservative as because experimental values are 1.20 to 4.25 times higher than Terzaghi's values. Ultimate bearing capacities obtained by Meyerhof's theory are still smaller being 65 to 78.50 percent of those obtained by Terzaghi's theory. This clearly shows that the use of Meyerhof's theory is too conservative and such will not be applicable for surface footings while Terzaghi's theory is conservative in the similar condition.

TABLE I

Values of Different Ultimate Loads at Different test conditions of Rectangular Footings

Test No.	Size of model footing cm×cm	Load at (e_x, e_y) or centre	Ultimate Load from test kg.	Ultimate Load from Terzaghi's Theory kg.	Ultimate load from Meyerhof's Theory kg.
1.	12.50×10	L/6, B/6	27.22	14.97	9.76
2.	,,	2L/6, B/6	14.52	4.63	3.29
3.	,,	L/6, 2B/6	9.98	3.72	2.82
4.	,,	2L/6, 2B/6	2.27	1.86	1.22
5.	,,	Centre	147.42	49.90	32.84
6.	15×10	L/6, B/6	54.43	17.69	12.39
7.	,,	2L/6, B/6	22.11	6.62	4.50
8.	,,	L/6, 2B/6	17.58	4.42	3.47
9.	,,	2L/6, 2B/6	3.97	2.21	1.54
10.	,,	Centre	185.98	59.88	41.60
11.	15×12.50	L/6, B/6	104.33	27.67	18.05
12.	,,	2L/6, B/6	35.15	8.30	5.90
13.	,,	L/6, 2B/6	29.48	6.89	5.28
14.	,,	2L/6, 2B/6	5.44	3.46	2.25
15.	,,	Centre	235.87	90.72	60.78

It is observed from Figures 7 and 8 that the vertical pressure decreases in asymtotic manner with the increase of depth for all the cases of rectangular and square footings. A pressure decrease of 9 to 59 percent is observed at double eccentricity of $e_x = L/6$, $e_y = B/6$, to that of centric

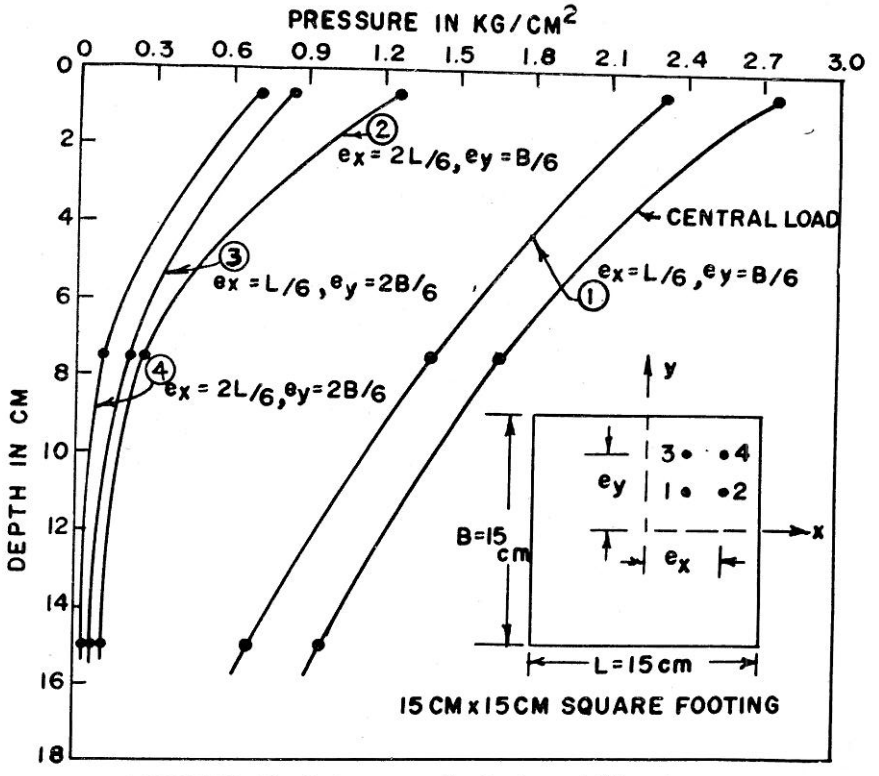

FIGURE 7 : Vertical pressure distributions at different e_x e_y.

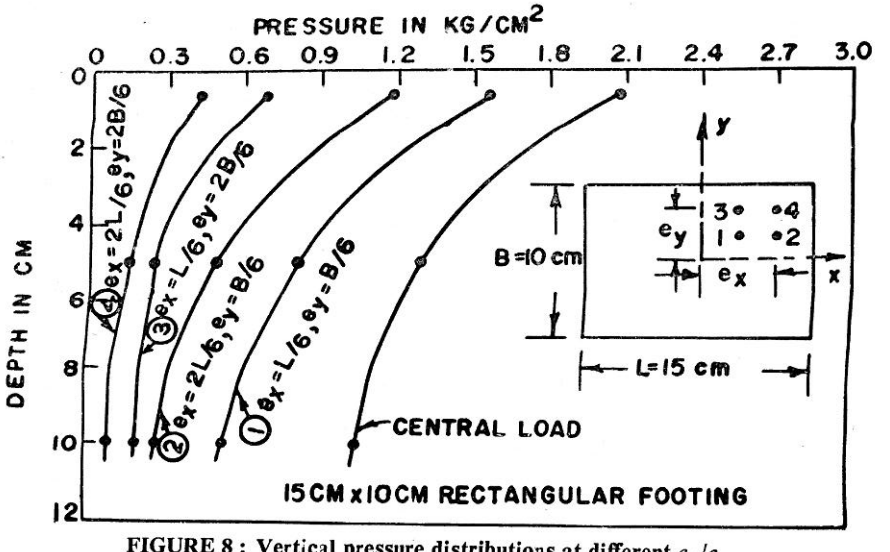

FIGURE 8 : Vertical pressure distributions at different e_x/e_y.

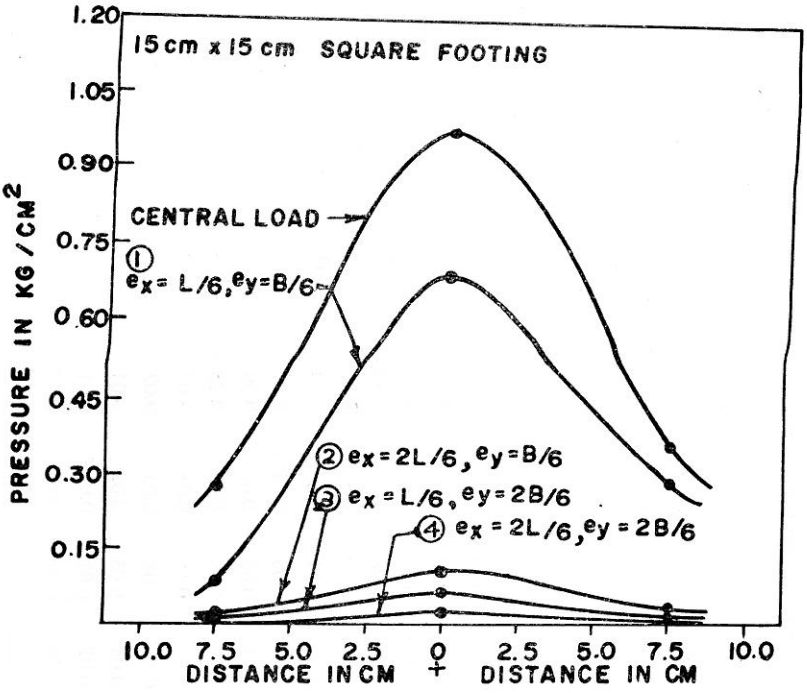

FIGURE 9 : Vertical pressure distributions at different e_x/e_y on horizontal plane.

load throughout the depth considered. The pressure decreases further with increased double eccentricities and at $e_x = 2L/6$, $e_y = 2B/6$, this is highly reduced to 70.50 to 98 percent for all the footings. In Table II, the observed pressures are compared with that of Boussinesq's equation which leads to very large stresses near the surface where loads are applied. The variation of pressures according to Boussinesq's equation is 106 to 220 times for centric load and nearly 9 to 30 times for double eccentricity of $e_x = 2L/6$, $e_y = 2B/6$, than the observed pressures near the surface. Thus it can be stated that Boussinesq's equation does not reveal the true stress close to proximity of the loading surface.

For all the cases of rectangular footings, it is observed from Figures 9 and 10 that the magnitude of vertical stresses on horizontal plane decreases with increase of double eccentricities and their nature of distributions are non-uniform. A pressure decrease of 17 to 82 percent is found throughout at double eccentricity of $e_x = L/6$, $e_y = B/6$, compared to that of centric load conditions. The pressure decreases further when double eccentricity increases and it is reduced beyond 91.50 percent when the double eccentricity is at $e_x = 2L/6$, $e_y = 2B/6$. Such reduction is attributed due to sharp decrease in ultimate load with increased double eccentricity. Between the two extreme horizontal pressures, in all the conditions of double eccentricities, it is observed that the pressures at the side of the double eccentricities are more, ranging from 50 to even 100 percent, than those at the other side of the double eccentricities.

TABLE II

Values of Different Vertical Pressures at Different test Conditions of Square Footings

Test No.	Size of model footing cm×cm	Load at (e_x, e_y) or Centre	Pressures in kg/sq cm									
			Cell No. 1		Cell No. 2		Cell No. 3		Cell No. 4		Cell No. 5	
			A	B	A	B	A	B	A	B	A	B
1.	15×15	L/6, B/6	2.32	127.96	1.40	0.89	0.69	0.22	0 28	0.13	0.09	0.13
2.	,,	2L/6, B/6	1.27	41.90	0.27	0.29	0.11	0.07	0.04	0.04	0.02	0.04
3.	,,	L/6, 2B/6	0.84	36.56	0.24	0.26	0.07	0.06	0.03	0.04	0.01	0.04
4.	,,	2L/6, 2B/6	0.72	13.92	0.10	0.10	0.03	0.03	0.00	0.01	0.00	0.01
5.	,,	Centre	2.76	327.64	1.66	2.29	0.98	0.58	0.35	0.33	0.28	0.34
6.	12.50×12.50	L/6, B/6	1.20	69.60	0.52	0.70	0.37	0.18	0.09	0.10	0.06	0.10
7.	,,	2L/6, B/6	0.69	20.95	0.19	0.21	0.11	0.05	0.04	0.03	0.01	0.03
8.	,,	L/6, 2B/6	0.36	16.87	0.13	0.17	0.08	0.04	0.04	0.03	0.01	0.03
9.	,,	2L/6, 2B/6	0.22	3.23	0.05	0.03	0.03	0.01	0.00	0.00	0.02	0.00
10.	,,	Centre	1.54	227.09	1.13	2.27	0.89	0.57	0.25	0.32	0.24	0.32
11.	10×10	L/6, B/6	0.45	20.81	0.25	0.33	0.16	0.08	0.07	0.05	0.03	0.05
12.	,,	2L/6, B/6	0.42	6.75	0.16	0.11	0.08	0.03	0.02	0.02	0.01	0.02
13.	,,	L/6, 2B/6	0.23	5.39	0.08	0.08	0.03	0.02	0.01	0.01	0.00	0.01
14.	,,	2L/6, 2B/6	0.16	1.35	0.04	0.02	0.02	0.01	0.01	0.00	0.00	0.00
15.	,,	Centre	0.74	163.12	0.47	2.56	0.35	0.64	0.17	0.37	0.16	0.37

A—From Test B—From Boussinesq's equation.

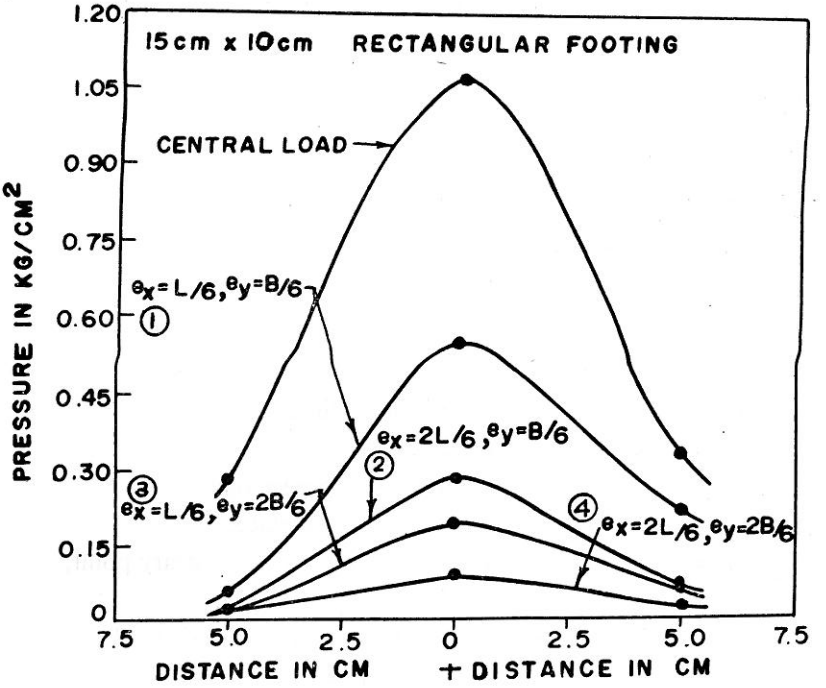

FIGURE 10 : Vertical pressure distributions at different e_x/e_y on horizontal plane.

Conclusions

From the critical studies of the test results and the discussions done, the following conclusions are drawn:—

1. Ultimate bearing capacity decreases very sharply with the increase of double eccentricities for any square and rectangular footings. Ultimate bearing capacity increases with the increase in area of both square and rectangular footing upto the double eccentricity of $e_x = L/6$, $e_y = B/6$, beyond which the size of footing has negligible effect on ultimate bearing capacity.
2. Terzaghi's theory for ultimate bearing capacity computation is conservative and Meyerhof's theory will not be applicable at the surface both for centric and double eccentric loads on cohesionless soil.
3. Boussinesq's equation does not reveal the true stress at the close proximity of the loading surface.
4. Magnitude of vertical stresses both in the vertical and horizontal planes decrease with the increase of double eccentricities.

Acknowledgement

The work reported herein is based on the M. Tech dissertation of the author. The facilities of the work were provided by the authorities of Indian Institute of Technology, Kharagpur. The author wishes to express his gratitude to Late Prof. S. K. Ghosh, of the same Institute for his

constant encouragement and valuable guidance in the course of the work. Thanks are also due to Dr. G. C. Mishra, Senior Lecturer in Civil Engineering, R. E. College, Rourkela, for his assistance in the preparation of the paper.

Notations

The following symbols are used in the paper :

c = cohesion,

γ = unit weight of soil mass,

L = length of footing,

B = width of footing,

L' = effective contact length of footing,

e = eccentricity at the base,

e_x, e_y = eccentricities in x and y axes respectively

z = depth below horizontal ground surface,

r = horizontal distance from z axes to an arbitrary point,

σ_z = vertical pressure at depth z,

q_e = ultimate bearing capacity under an eccentric load,

q_d = ultimate bearing capacity at general shear failure,

N_γ = bearing capacity factor, and

N_{cq}, $N_{\gamma q}$ = resultant bearing capacity factors.

References

BALLA, A (1962), "Bearing capacity of foundations", *Journal of Soil Mechanics and Foundation Division, ASCE*, Vol. SM 5-89 pp 13-34.

BELL, A.L. (1915), "The lateral pressure and resistance of clay and supporting power of clay foundation", Minutes of *Proceedings of the Institution of Civil Engineers, London*, Paper No. 4131.

HANSEN, J.B. (1961), "A general formula for bearing capacity", *Danish Geotech, Inst. Bull. 11, Copenhagen.*

JUMIKIS, A.R. (1965), "*Soil Mechanics*", D. Van Nostrand Co. Inc., London.

MEYERHOF, G.G. (1951), "The ultimate bearing capacity of foundations" *Geotechnique*, Vol. II, No. 4, pp 301-331.

MEYERHOF, G.G. (1953), "The ultimate bearing capacity of foundation under centric and eccentric loads", *Proceedings of 3rd International Conference on Soil Mech. and Foundation Engg.*, Vol. I, Zurich pp 440.

SKEMPTON, A.W. (1951), "The bearing capacity of clays" *Building Research Congress Div.*, I, London.

TENG, W.C. (1962), "*Foundation Design*", Prentice Hall Inc, New Jersey.

TERZAGHI, K. (1943), "*Theoretical Soil Mechanics*" John Willey and Sons Inc., New York, Chapter-8.

VICTOR, D. JOHNSON (1958), "Beams on Elastic foundations", *M. Tech. Thesis in Structural Engineering*, Indian Institute of Technology, Kharagpur.

Appendix

Method of Evaluation

These were done in the following steps and a typical example is presented below for 15 cm × 15 cm square footing of double eccentricities $e_x = 2L/6 = 5$ cm, $e_y = B/6 = 2.50$ cm ;

(*a*) The load settlement curve was drawn with tangent intersection method from which ultimate load was 35.38 kg (Figure 3).

(*b*) The load vs. corresponding pressures in the cells were drawn in Figure 11. The corresponding pressure in each cell was found out to give pressures at the ultimate load condition.

(*c*) Ultimate bearing capacity of footing under double eccentric load applied at the surface of cohesionless soil was calculated from the assumed minimum effective contact area $L'B'$.

(*i*) Applying Terzaghi's theory ($c = 0$, $z = 0$)

$L' = L - 2e_x = 5$ cm, $\quad B' = B - 2e_y = 10$ cm.

$\gamma = 1.65$ gm/cc, $\quad N_\gamma = 46$ for $\phi = 55°$

$q_d = 9.98$ kg.

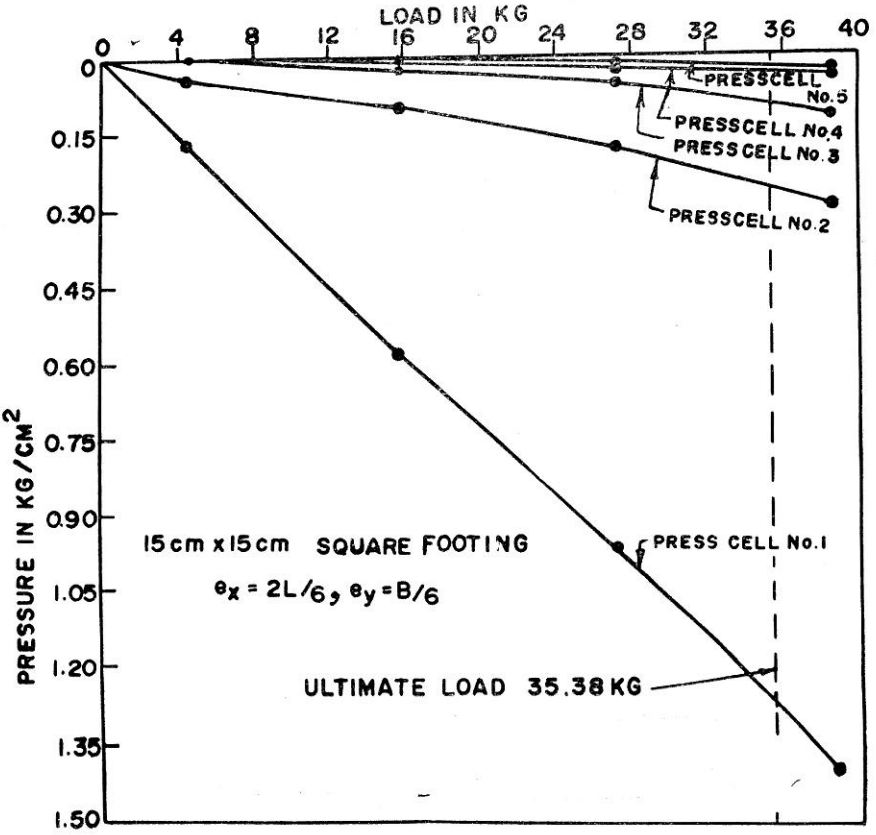

FIGURE 11 : Load vs corresponding pressures in the pressure cells

(*ii*) Applying Meyerhof's theory ($c = 0$, $z = 0$)

L', B' and γ as in (*i*)

$N_\gamma = 40$ for $\phi = 35°$

Correction for shape factor applied to

$N_\gamma = 0.5\ (1 - 0.3 \times 5/10) = 0.425$

$$q_d = 7.35 \text{ kg.}$$

(*d*) Regarding the pressure distributions Boussinesq's equation was applied. Accordingly pressure at different locations worked out as follows, with ultimate load of 35.38 kg.

Cell No.	z in cm	r in cm	σ_z in kg/cm^2
1	0.635	0	41.900
2	7.500	0	0.290
3	15.000	0	0.073
4 and 5	15.000	7.50	0.041